Where do moving punctures go?

Mark Hannam, Sascha Husa, Bernd Brügmann, José A González, Ulrich Sperhake

Theoretical Physics Institute, University of Jena, 07743 Jena, Germany

Niall Ó Murchadha

Physics Department, University College Cork, Ireland

Abstract. Currently the most popular method to evolve black-hole binaries is the "moving puncture" method. It has recently been shown that when puncture initial data for a Schwarzschild black hole are evolved using this method, the numerical slices quickly lose contact with the second asymptotically flat end, and end instead on a cylinder of finite Schwarzschild coordinate radius. These slices are stationary, meaning that their geometry does not evolve further. We will describe these results in the context of maximal slices, and present time-independent puncture-like data for the Schwarzschild spacetime.

1. Introduction

Recent breakthroughs in numerical relativity have made black-hole binary evolutions routine for many research groups. The easiest method to implement, and currently the most popular, is the "moving puncture" approach. Here one begins with initial data that possess a Brill-Lindquist wormhole topology [1] and each asymptotic end is compactified to a single point (puncture) on R^3 at the price of a coordinate singularity. Punctures are technically appealing because they represent black holes on R^3 without excision, the initial-data slices avoid the curvature singularity of each black hole, and it is well understood how to construct puncture initial data for any number of boosted, spinning black holes [2, 3].

The numerical evolution of puncture data is not so well understood. Successful numerical techniques have been found only by trial and error. These include the choice of formulation of the evolution equations, gauge conditions and, most importantly, the treatment of the coordinate singularity at each puncture. Early "fixed puncture" evolutions [4, 5] factored the singularity into a fixed analytically prescribed conformal factor and a regular function that is evolved numerically, and used gauge conditions that prevented the punctures from moving across the grid. These methods met with some success, but long-term stable evolutions of general configurations of (especially orbiting) black-hole binaries were not achieved. Puncture evolutions received very little analytic attention, but it is interesting for the results we will describe here that the only detailed analytic study of the properties of fixed-puncture evolutions [6, 7], applied to the Schwarzschild spacetime, showed that such evolutions would never reach a stationary state: nontrivial evolution of the slices of Schwarzschild would continue indefinitely.

Recently two groups [8, 9] independently introduced similar methods to deal with the puncture singularities. The singular conformal factor ψ is evolved without any analytic assumptions (by evolving a new variable, either $\chi = \psi^{-4}$ [8] or $\phi = \ln \psi$ [9]), and the punctures

are able to move on the numerical grid. These methods have met with spectacular success, and the "moving puncture" method is now the most popular method for evolving black-hole binaries — of the eight codes reported to have successfully performed long-term evolutions of several orbits [10, 8, 9, 11, 12, 13, 14, 15], six use moving punctures.

A number of questions were raised after the first moving-puncture results were published. What happens to the punctures during the evolution? Do they continue to represent compactified infinities? Does the evolution reach a final, stationary state, or do gauge dynamics persist, as in the fixed-puncture case? And, crucially, does the method accurately describe the spacetime, or does it rely on numerical errors near the under-resolved punctures, implying that it may fail when probed at higher resolutions or for longer evolutions?

These questions were answered by Hannam *et al* in [16], who studied moving-puncture evolutions of the Schwarzschild spacetime. The answers were, in short, that the evolution quickly reaches a stationary state. The slices no longer extend to the other asymptotically flat end, but instead end on a surface of finite Schwarzschild coordinate radius. For the version of 1+log slicing that the authors considered, the stationary slice ends at $R = 1.3M$. This point represents a throat and, although at a finite Schwarzschild coordinate radius, it is an infinite proper distance from the horizon. The authors also solve the stationary Einstein equations in spherical symmetry with the 1+log slicing condition, and show that the numerical evolution accurately reproduces this solution, demonstrating that the moving-puncture method is capable of accurately describing a black-hole spacetime, and the region near the "puncture" is not under-resolved.

In this article we will describe these effects in the context of slices of Schwarzschild that are maximal in the initial and final states. The advantage of considering maximal slices is that analytic closed-form expressions exist for these initial and final states. We may also easily construct time independent initial data for a Schwarzschild black hole, which allow us to study in more detail the numerical accuracy of the moving-puncture method.

2. Puncture evolutions of the Schwarzschild spacetime

Following the standard 3+1 decomposition of Einstein's equations [17, 18] we write the spacetime metric as

$$ds^2 = -\alpha^2 dt^2 + \gamma_{ij} \left(dx^i + \beta^i dt\right) \left(dx^j + \beta^j dt\right), \tag{1}$$

where α is the lapse function, β^i is the shift vector and γ_{ij} is the spatial metric on one slice. The data on each time slice are (γ_{ij}, K_{ij}), where the extrinsic curvature is given by

$$K_{ij} = \frac{1}{2\alpha} \left(\nabla_i \beta_j + \nabla_j \beta_i - \partial_t \gamma_{ij}\right). \tag{2}$$

The data can be further decomposed by conformally relating the spatial metric γ_{ij} to a background metric $\tilde{\gamma}_{ij}$ via a conformal factor ψ, and providing conformal weights to the trace and tracefree parts of the extrinsic curvature [18],

$$\begin{aligned}
\gamma_{ij} &= \psi^4 \tilde{\gamma}_{ij} \\
K_{ij} &= \psi^{-2} \tilde{A}_{ij} + \frac{1}{3}\gamma_{ij} K.
\end{aligned}$$

These data must satisfy constraint equations on each slice, and the data on consecutive slices are related by evolution equations.

It is in this context that puncture initial data are usually constructed. We will restrict ourselves to the Schwarzschild solution. The standard Schwarzschild metric is

$$ds^2 = -\left(1 - \frac{2M}{R}\right) dt^2 + \left(1 - \frac{2M}{R}\right)^{-1} dR^2 + R^2(d\theta^2 + \sin^2\theta d\phi^2). \tag{3}$$

If we make the coordinate transformation $R = \psi^2 r$, where

$$\psi = 1 + \frac{M}{2r}, \tag{4}$$

the Schwarzschild metric becomes

$$ds^2 = -\left(\frac{1 - \frac{M}{2r}}{1 + \frac{M}{2r}}\right)^2 dt^2 + \left(1 + \frac{M}{2r}\right)^4 \left(dr^2 + r^2 d\Omega^2\right). \tag{5}$$

In these "isotropic" coordinates, the spatial metric takes the form $\gamma_{ij} = \psi^4 \tilde{\gamma}_{ij}$, and the background spatial metric is the flat metric, $\tilde{\gamma}_{ij} = f_{ij}$.

One important feature of isotropic coordinates is that they do not reach the physical singularity at $R = 0$. For large r we see that $R \to \infty$, but for small r we also see that $R \to \infty$. There is a minimum of $R = 2M$ at $r = M/2$. We now have two copies of the space outside the event horizon, $R > 2M$, and the two spaces are connected by a wormhole (Einstein-Rosen bridge) with a throat at $R = 2M$. We refer to the second asymptotically flat end (at $r = 0$) as the puncture. Schwarzschild R as a function of isotropic r is shown in Figure 2.

The Schwarzschild metric in isotropic coordinates is explicitly time independent: if we evolve γ_{ij} and K_{ij} using the lapse and shift $\alpha = (1 - M/2r)/(1 + M/2r)$, $\beta^i = 0$, we will find that γ_{ij} and K_{ij} do not change. This is not to say that nothing will happen in a *numerical* evolution: the lapse function is negative for $r < M/2$, and negative lapses usually lead to numerical instabilities. However, the Schwarzschild metric in isotropic coordinates is analytically time independent.

We are free to slice the spacetime in some other way, i.e., to make a different choice of lapse and shift. This will lead to a nontrivial evolution of (γ_{ij}, K_{ij}). The spacetime remains the stationary Schwarzschild spacetime, but the coordinates will no longer be time independent.

One simple choice for initial lapse and shift is $\alpha = 1$ and $\beta^i = 0$. If we maintain these choices throughout the evolution, however, the slices will hit the singularity in finite time, and we therefore choose to evolve the gauge in such a way that the slices continue to avoid the singularity. Here we will choose the gauge conditions popular in evolutions of black-hole binary puncture data. The lapse is evolved with one of two variants of 1+log slicing [19],

$$\partial_t \alpha = -2\alpha K \tag{6}$$

$$\partial_t \alpha = -2\alpha K + \beta^i \partial_i \alpha, \tag{7}$$

and we evolve the shift vector with a $\tilde{\Gamma}$-freezing condition [20],

$$\partial_t \beta^i = \frac{3}{4} B^i, \tag{8}$$

$$\partial_t B^i = \partial_t \tilde{\Gamma}^i - \eta B^i, \tag{9}$$

where $\tilde{\Gamma}^i = -\partial_j \tilde{\gamma}^{ij}$. The lapse choice (7) was analyzed in [16], while here we will consider (6). This choice has the attractive property that a stationary state will be maximal ($2\alpha K = 0 \Rightarrow K = 0$).

2.1. Numerical slices

Now let us consider evolving isotropic Schwarzschild data with the gauge choices (6), (9) and (2). Most current work uses the BSSN reformulation of the 3+1 equations [21, 22], and the BSSN system has also been used to obtain the results shown here, using the BAM code [14]. (See also the articles by Sperhake and Gonzalez in these proceedings.) However, the BSSN system is irrelevant to the evolution of the geometry. Only gauge conditions with the properties of (6) -
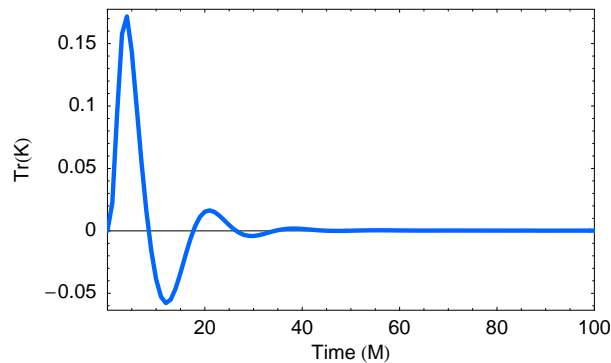
Figure 1. The value of K on the horizon $R = 2M$ as a function of time, for a moving-puncture evolution of Schwarzschild initial data. In this case the evolution reaches a stationary state.

(9) are necessary. (That isn't to say that some other formulation will be numerically stable; but we are interested in how the geometry evolves due to the gauge conditions, not the numerical properties of a particular evolution system.)

Having said that, the one element of the BSSN equations that must be singled out if we are to discuss "fixed" versus "moving" punctures is the treatment of the conformal factor, ψ, which is an independent evolution variable in the BSSN system. The apparent problem with the conformal factor is that it diverges at the puncture, and will presumably behave badly if evolved directly. In "fixed puncture" evolutions one avoids this problem by writing the initial isotropic Schwarzschild conformal factor as

$$\psi = \left(1 + \frac{M}{2r}\right) f, \tag{10}$$

where $f = 1$ at the beginning of the evolution, and then evolving only f (or, rather, $\ln f$), and leaving the divergent part fixed. The method is tailored so that the wormhole topology remains throughout the evolution. This means that even in black-hole binary simulations, where the black holes have physical motion, the punctures are kept fixed on the grid [4, 5].

It was pointed out in [6] that Schwarzschild evolutions in such a setup never reach a stationary state. One way of seeing this is that if they did, the lapse would have to pass through zero at the throat, and the slicing choices used in puncture evolutions preclude this. The same problem was noted in attempts to construct quasi-equilibrium puncture data for black-hole binaries with an everywhere positive lapse [23].

Now consider the "moving-puncture" method. Here one does not assume anything about the form of ψ during the evolution. We simply evolve either $\phi = \ln \psi$ [9] or $\chi = \psi^{-4}$ [8], both of which behave sufficiently well at the puncture to allow stable evolutions. (This may be a surprise for the choice $\phi = \ln \psi$, which diverges logarithmically at the puncture, but it turns out that this divergence is not strong enough to break the method.)

Figure 1 shows the value of K at the horizon $(R = 2M)$ during a moving-puncture evolution. On the initial slice $K = 0$. As the evolution progresses K varies, but settles back to a maximal slice after about $40M$, and remains there. After this time a check of other invariant quantities reveals that the evolution has reached a stationary state.

Now let us look at the evolution of the topology. Initially, the slice connects two asymptotically flat ends. This is clearly seen in Figure 2, which shows the Schwarzschild radial coordinate R as a function of numerical radial coordinate r.

Figure 3 shows $R(r)$ at times $t = 0, 1, 2, 3M$ in a numerical evolution. We see that the numerical slice quickly loses contact with the second asymptotically flat end. The slice initially
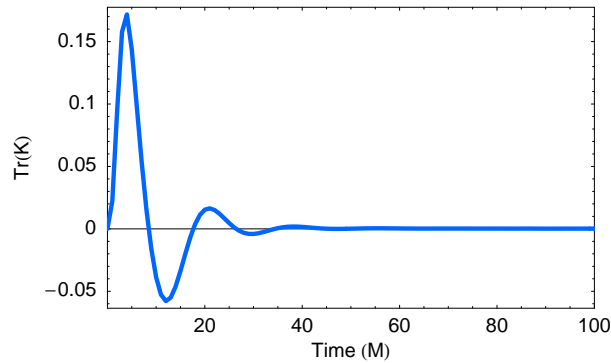
Figure 2. The Schwarzschild radial coordinate R as a function of numerical distance r for the initial data.
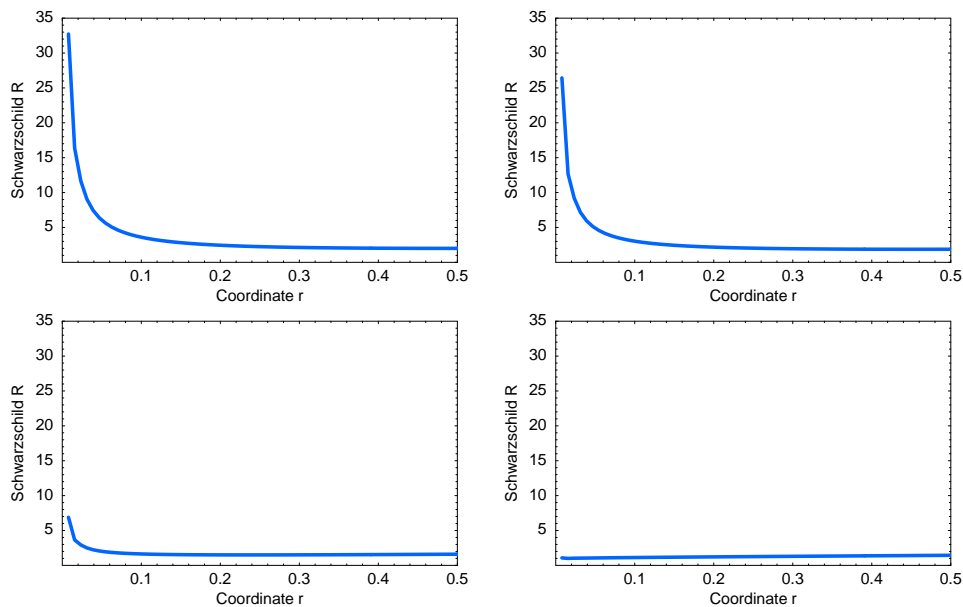

Figure 3. The Schwarzschild radial coordinate R as a function of numerical distance r at times $T = 0, 1M, 2M, 3M$ in the top-left, top-right, bottom-left and bottom-right figures. We see that the numerical slice loses contact with the second asymptotically flat end.

extends to $R \rightarrow \infty$ as $r \rightarrow 0$, but during evolution quickly retracts to a finite value of the Schwarzschild radial coordinate. Figure 4 shows the value of R at $r = 0$ as a function of time. After some complicated oscillation, the end of the numerical slice settles at $R = 3M/2$, again after about $40M$.

In order for the slice to end at $R = 3M/2$, the nature of the singularity in the conformal factor ψ must change. In the initial data ψ diverges as $1/r$ at the puncture. By the time the evolution reaches a stationary state, ψ diverges as $1/\sqrt{r}$. In fact, near the puncture it will look like $\psi \sim \sqrt{3M/2r}$ and $R = \psi^2 r \rightarrow 3M/2$. In the case of the modified 1+log slicing (7) studied in [16], the slice ends at $R = 1.3M$, and $K \neq 0$. The numerical and analytic descriptions of that slice were found to be in excellent agreement.
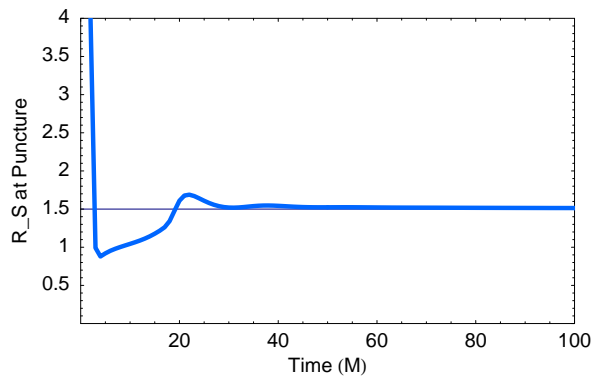
Figure 4. The Schwarzschild radial coordinate R at the puncture $r = 0$ as a function of time. The end of the slice settles at $R = 3M/2$ after about $40M$ of evoluution.

2.2. Analytic maximal slices

We may understand this result by comparison with the analytic result in the 1973 paper of Estabrook *et al* [24]. That paper contains an analytic maximal slicing of the Schwarzschild spacetime for all time. The $t \to 0$ limit of the Estabrook *et al* slicing is

$$
\begin{aligned}
\gamma_{rr} &= \left(1 - \frac{2M}{R}\right)^{-1} \\
\beta^r &= 0 \\
\alpha &= 1.
\end{aligned}
$$

If we transform to isotropic coordinates, we have precisely the initial data that were used in our numerical evolution. Our final stationary state is also a maximal slice, and therefore should represent (at least part of) the $t \to \infty$ Estabrook *et al* solution, which is

$$
\gamma_{rr} = \left(1 - \frac{2M}{R} + \frac{C^2}{R^4}\right)^{-1}, \tag{11}
$$

$$
\beta^r = \frac{\alpha C}{R^2}, \tag{12}
$$

$$
\alpha = \sqrt{1 - \frac{2M}{R} + \frac{C^2}{R^4}}, \tag{13}
$$

with $C = 3\sqrt{3}/4$. In this solution we see that the lapse is zero at $R = 3M/2$: the slice ends there, just as in our numerical evolution! In a Kruskal diagram, the throat is an infinitely long 3-cylinder [24]. The same effect was seen in the numerical evolutions by Estabrook *et al* in 1973, with a 1D code that required only 25 grid points. The remarkable feature of the moving-puncture technique is that it finds this time-independent slice (in slightly different coordinates) with the cylinder at $R = 3M/2$ located at the origin of the numerical coordinate system, and finds analogous slices in general configurations of multiple black holes. As attractive as such an evolution system is, all of the tools of the moving-puncture method were motivated by other considerations, and there was no deliberate attempt to "find" slices like (11)– (13). In the next section we will present Schwarzschild puncture initial data that *are* motivated by the time-independent analytic solution.
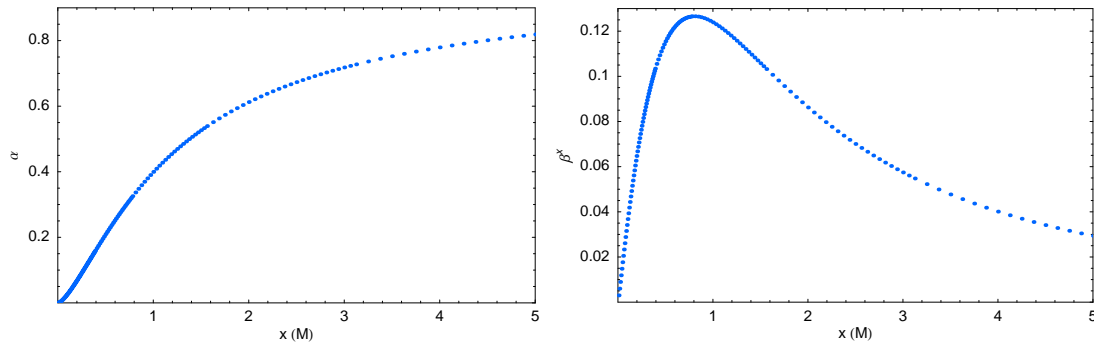
Figure 5. The lapse function and x-component of the shift vector for time-independent puncture data for the Schwarzschild spacetime, based on the $t \to \infty$ limit of the Estabrook *et al* solution.

3. "Cylindrical" initial data

Motivated by the analytic Estabrook *et al* solution, we may attempt to construct stationary initial data, i.e., data that do not change when evolved with our 1+log and $\tilde{\Gamma}$-driver gauge conditions.

To do this in a way that is most transparently related to the moving-puncture method, we can conformally relate the $t \to \infty$ Estabrook *et al* spatial metric to a flat metric with a conformal factor that behaves as $\psi \sim \sqrt{3M/2r}$ at the puncture. This conformal factor must also behave as $\psi \sim 1 + M/2r$ as $r \to \infty$, in order to give the correct ADM mass of the spacetime. We choose an ansatz that satisfies these two conditions, and add to it a correction function such that the Hamiltonian constraint is satisfied, in analogy to the standard puncture method for black-hole binary initial data [2]. The Hamiltonian constraint becomes an elliptic equation for the correction function u, which can be solved in this case with a 1D code. Having found the appropriate conformal factor ψ, we can reconstruct the background lapse and shift, and background extrinsic curvature $\tilde{A}_{ij}$, and use these as initial data for a dynamical evolution. The lapse and x-component of the shift vector are shown in Figure 5.

These data are indeed stationary: when we evolve them with the moving-puncture method we see no obvious change in the grid functions with time. A calculation of the error as a function of time (the difference between the initial data and the evolved variables) shows that there *is* some nontrivial evolution, but that this converges away with resolution. This is shown in Figure 6, where we see that numerical noise emerges from the puncture. It is possible that this noise is largely due to the error in taking finite-difference derivatives across the puncture of variables that are not sufficiently smooth there. (For example, the lapse behaves like $\alpha \sim |r|$ across the puncture.) However, the noise is small, it does not grow with time, and it does not cause the simulation to crash. We also see noise propagating in from the other boundary in the second panel in Figure 6, which does not converge away. This is due to the physically incorrect outer boundary conditions.

These stationary data provide an excellent testbed for numerical evolutions: knowing the correct analytic values of all evolution variables, we can carefully monitor all errors in a simulation. It may also be possible to generalize this construction to produce data of a similar type for black-hole binaries. The physical quality of the data will depend on the choices of the free data in our initial-data construction, but even if they do not have any better physical properties than the Bowen-York data currently used in most moving-puncture simulations, they would represent black holes in coordinates in which the initial gauge dynamics would be minimized, in a similar fashion to the "quasi-equilibrium" conformal thin-sandwich initial-data sets (see, for example, [25] and [13]).
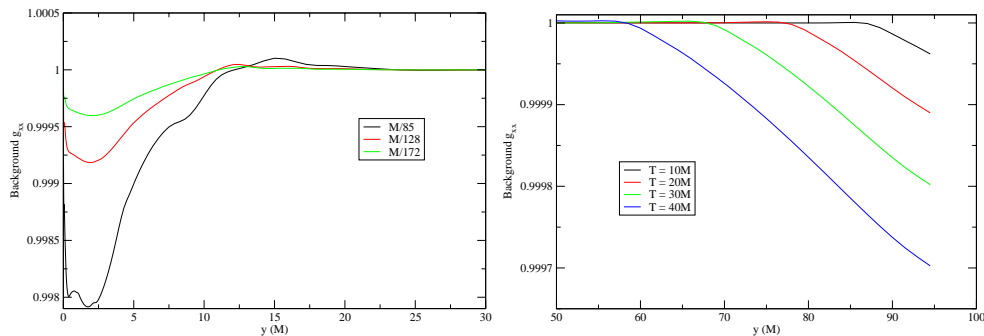
Figure 6. Errors in the evolution of the time-independent Schwarzschild initial data. The left panel shows the error in $\tilde{\gamma}_{xx}$ after $20M$ of evolution, with grid resolutions of $h = M/85, M/128, M/172$. The right panel shows the error that has propagated in from the outer boundary after $T = 10M, 20M, 30M, 40M$.

4. Conclusion

We have described the evolution of the geometry of puncture initial data in the "moving puncture" method in the context of asymptotically maximal slices of the Schwarzschild spacetime. This description complements the picture in terms of the 1+log slicing (7) described in [16]. The main features of these evolutions are that the numerical slices lose contact with the second asymptotically flat end that is present in the initial data. The slices instead end on a cylinder of finite Schwarzschild radial coordinate (but infinite proper distance) inside the event horizon. As a result, the conformal factor that initially diverged as $1/r$ at the puncture now has a milder divergence of $1/\sqrt{r}$. The numerical evolution reaches a stationary state in about $40M$, and the final stationary state can be described by the $t \to \infty$ limit of the Estabook *et al* solution. Knowledge of the analytic solution in turn allows us to construct initial data that is unchanging in a numerical evolution, and provides a convenient experimental environment to test the accuracy and stability of numerical codes. In addition, these "cylindrical data" may provide insight into a method to produce black-hole binary initial data in coordinates better suited to numerical evolutions.

References

[1] Brill D S and Lindquist R W 1963 *Phys. Rev.* **131**(1) 471–476
[2] Brandt S and Brügmann B 1997 *Phys. Rev. Lett.* **78**(19) 3606–3609
[3] Dain S 2002 *Lect. Notes Phys.* **604** 161–182
[4] Brügmann B 1999 *Int. J. Mod. Phys.* D **8** 85
[5] Alcubierre M, Benger W, Brügmann B, Lanfermann G, Nerger L, Seidel E and Takahashi R 2001 *Phys. Rev. Lett.* **87** 271103
[6] Reimann B and Brügmann B 2004 *Phys. Rev.* D **69** 044006
[7] Reimann B and Brugmann B 2004 *Phys. Rev.* D **69** 124009
[8] Campanelli M, Lousto C O, Marronetti P and Zlochower Y 2006 *Phys. Rev. Letter* **96** 111101
[9] Baker J G, Centrella J, Choi D I, Koppitz M and van Meter J 2006 *Phys. Rev. Lett.* **96** 111102
[10] Pretorius F 2005 *Phys. Rev. Lett.* **95** 121101
[11] Herrmann F, Shoemaker D and Laguna P 2006 *Preprint* gr-qc/0601026
[12] Sperhake U 2006 *Preprint* gr-qc/0606079

[13] Scheel M A *et al.* 2006 *Phys. Rev.* D **74** 104006
[14] Brügmann B, González J A, Hannam M, Husa S, Sperhake U and Tichy W 2006 *Preprint* `gr-qc/0610128`
[15] Pollney D July 2006 Presented at the *New Frontiers in Numerical Relativity* meeting, Golm
[16] Hannam M, Husa S, Pollney D, Brügmann B and Ó Murchadha N 2006 *Preprint* `gr-qc/0606099`
[17] Arnowitt R, Deser S and Misner C W 1962 *Gravitation: An introduction to current research* ed L Witten (New York: John Wiley) pp 227–265
[18] York J W 1979 *Sources of gravitational radiation* ed L L Smarr (Cambridge: Cambridge University Press) pp 83–126
[19] Bona C, Massó J, Seidel E and Stela J 1997 *Phys. Rev.* D **56** 3405–3415
[20] Alcubierre M, Brügmann B, Diener P, Koppitz M, Pollney D, Seidel E and Takahashi R 2003 *Phys. Rev.* D **67** 084023
[21] Shibata M and Nakamura T 1995 *Phys. Rev.* D **52** 5428
[22] Baumgarte T W and Shapiro S L 1999 *Phys. Rev.* D **59** 024007
[23] Hannam M D, Evans C R, Cook G B and Baumgarte T W 2003 *Phys. Rev.* D **68** 064003
[24] Estabrook F, Wahlquist H, Christensen S, DeWitt B, Smarr L and Tsiang E 1973 *Phys. Rev.* D **7**(10) 2814–2817
[25] Cook G B and Pfeiffer H P 2004 *Phys. Rev.* D **70** 104016